ENHANCHEMENT OF IONIZATION EFFICIENCY OF ACCEPTORS BY THEIR EXCITED STATES IN HEAVILY DOPED P-TYPE GaN AND WIDE BANDGAP SEMICONDUCTORS

Hideharu Matsuura
Department of Electro-Communication University,
18-8 Hatsu-cho, Neyagawa, Osaka 572-8530, Japan

The temperature dependencies of the hole concentrations $p(T)$ for heavily Mg-doped GaN, Al-implanted 4H-SiC and Al-doped 6H-SiC, and lightly Al-doped 6H-SiC are obtained from Hall-effect measurements. The density and energy levels (ΔE_A) of acceptors are determined by the graphical peak analysis method (free carrier concentration spectroscopy) from $p(T)$. Since ΔE_A is deep, it is found that a distribution function including the influence of the excited states of acceptors is necessary to the analysis of $p(T)$ for the heavily doped samples. Moreover, it is proved that the excited states enhance the ionization efficiency of acceptors in the heavily doped case.

INTRODUCTION

GaN, SiC and diamond have been attractive wide bandgap semiconductors for devices operating at high powers, high frequencies, and high temperatures. In their p-type semiconductors, the energy levels (ΔE_A) of acceptors are experimentally reported to be deep (1,2). According to the hydrogenic model (3), on the other hand, a ground state level corresponding to a theoretical ΔE_A of a substitutional acceptor in GaN, SiC or diamond is also expected to be deep because of its dielectric constant (ε_s) lower than ε_s of Si as well as its hole effective mass (m_h^*) heavier than its electron effective mass. For example, ΔE_A for SiC is calculated as 146 meV, and the first excited state level (ΔE_2) is estimated to be 36 meV that is close to ΔE_A of B in Si. Therefore, the excited states are considered to affect the temperature dependence of the hole concentration $p(T)$ in p-type wide bandgap semiconductors.

In this article, a distribution function suitable for deep acceptors in heavily doped p-type GaN and SiC is investigated using $p(T)$ obtained from Hall-effect measurements. Since the Fermi levels in heavily doped samples are located between the valence band maximum (E_V) and ΔE_A, there are a lot of holes at the excited states of acceptors. This indicates that the distribution function for deep acceptors should include the influence of the excited states of acceptors. Therefore, we here consider two

distribution functions; (i) the Fermi-Dirac distribution function $f_{FD}(\Delta E_A)$ not including the influence and (ii) our proposed distribution function $f(\Delta E_A)$ including it (4-7). In lightly doped semiconductors where the Fermi levels are far from E_V, on the other hand, $f_{FD}(\Delta E_A)$ is assumed to be appropriate for determining the acceptor density (N_A) and ΔE_A from $p(T)$ (7,8). Therefore, in order to determine N_A and ΔE_A from $p(T)$, we here apply the graphical peak analysis method (free carrier concentration spectroscopy; FCCS) (4-15), which can determine N_A and ΔE_A using any distribution function such as $f_{FD}(\Delta E_A)$ or $f(\Delta E_A)$. Moreover, we report on our investigation as to how the excited states affect the ionization efficiency of deep acceptors.

DISTRIBUTION FUNCTION FOR DEEP ACCEPTORS

$f_{FD}(\Delta E_A)$ is described as (16)

$$f_{FD}(\Delta E_A) = \frac{1}{1 + g_A \exp\left(\frac{\Delta E_A - \Delta E_F(T)}{kT}\right)}, \quad [1]$$

where $\Delta E_F(T)$ is the Fermi level measured from E_V, g_A is the acceptor degeneracy factor of 4, k is the Boltzmann constant, and T is the absolute temperature.

On the other hand, $f(\Delta E_A)$ is given by (4-7)

$$f(\Delta E_A) = \frac{1}{1 + g_A(T)\exp\left(\frac{\Delta E_A - \Delta E_F(T)}{kT}\right)}, \quad [2]$$

where

$$g_A(T) = g_A\left[1 + \sum_{r=2} g_r \exp\left(\frac{\Delta E_r - \Delta E_A}{kT}\right)\right]\exp\left(-\frac{\overline{E_{ex}(T)}}{kT}\right), \quad [3]$$

g_r is the $(r-1)$th excited state degeneracy factor of r^2, ΔE_r is the difference in energy between E_V and the $(r-1)$th excited state level, described as

$$\Delta E_r = 13.6\frac{m_h^*}{m_0 \varepsilon_s^2} \cdot \frac{1}{r^2} \quad [\text{eV}], \quad [4]$$

$\overline{E_{\mathrm{ex}}(T)}$ is an ensemble average energy of the acceptor and excited state levels, given by

$$\overline{E_{\mathrm{ex}}(T)} = \frac{\sum_{r=2} (\Delta E_{\mathrm{A}} - \Delta E_r) g_r \exp\left(-\frac{\Delta E_{\mathrm{A}} - \Delta E_r}{kT}\right)}{1 + \sum_{r=2} g_r \exp\left(-\frac{\Delta E_{\mathrm{A}} - \Delta E_r}{kT}\right)}, \quad [5]$$

and m_0 is the free space electron mass.

FREE CARRIER CONCENTRATION SPECTROSCOPY

Basic Concept

Deep level transient spectroscopy (DLTS) (17), isothermal capacitance transient spectroscopy (ICTS) (18), and some methods (19,20) can uniquely determine the densities and energy levels of traps in semiconductors or insulators, because each peak in the signal corresponds one-to-one to a trap. For example, the ICTS signal is defined as $S(t) \equiv t\mathrm{d}C(t)^2/\mathrm{d}t$, where $C(t)$ is the transient capacitance after a reverse bias is applied for a pn diode or a Schottky barrier diode. Since $S(t)$ is theoretically described as the sum of $N_i e_i t \exp(-e_i t)$, it has a peak value of $N_i \exp(-1)$ at a peak time of $t_{\mathrm{peak}i} = 1/e_i$. Here, N_i and e_i are the density and emission rate of an ith trap. Therefore, the function of $N_i e_i t \exp(-e_i t)$ plays an important role in the ICTS analysis.

In order to analyze $p(T)$, we introduced the function theoretically described as the sum of $N_{\mathrm{A}i} \exp(-\Delta E_{\mathrm{A}i}/kT)/kT$ (9-12), where $N_{\mathrm{A}i}$ and $\Delta E_{\mathrm{A}i}$ are the density and energy level of an ith acceptor species. The function of $N_{\mathrm{A}i} \exp(-\Delta E_{\mathrm{A}i}/kT)/kT$ has a peak at $T_{\mathrm{peak}i} = \Delta E_{\mathrm{A}i}/k$, which does not apply to all acceptor species in a limited temperature range of the measurement. If you introduce a function in which a peak appears at $T_{\mathrm{peak}i} = (\Delta E_{\mathrm{A}i} - E_{\mathrm{ref}})/k$, you can shift the peak temperature to the measurement temperature range by changing the parameter E_{ref}. This indicates that you can determine $N_{\mathrm{A}i}$ and $\Delta E_{\mathrm{A}i}$ in a wide range of acceptor levels even within a limited measurement temperature range. Therefore, the function to be evaluated should be approximately described as the sum of $N_{\mathrm{A}i} \exp[-(\Delta E_{\mathrm{A}i} - E_{\mathrm{ref}})/kT]/kT$. It should be noted that $N_{\mathrm{A}i}$ and $\Delta E_{\mathrm{A}i}$ determined by this method are independent of E_{ref}.

Theoretical Consideration

FCCS is a graphical peak analysis method for determining the densities and energy levels of acceptor species in a semiconductor from $p(T)$, even when the number of acceptor species included in the semiconductor is unknown. Using an experimental $p(T)$, the FCCS signal is defined as (4-8,13-15)

$$H(T,E_{\mathrm{ref}}) \equiv \frac{p(T)^2}{(kT)^{5/2}} \exp\left(\frac{E_{\mathrm{ref}}}{kT}\right). \qquad [6]$$

Although FCCS can be applied to any nondegenerate semiconductor including several types of acceptor species, donor species and traps, we here focus on a p-type semiconductor doped with one type of acceptor species. From the charge neutrality condition, $p(T)$ is given by (16)

$$p(T) = N_{\mathrm{A}} F(\Delta E_{\mathrm{A}}) - N_{\mathrm{D}} \qquad [7]$$

in the temperature range in which the electron concentration is much less than $p(T)$, where $F(\Delta E_{\mathrm{A}})$ represents $f_{\mathrm{FD}}(\Delta E_{\mathrm{A}})$ or $f(\Delta E_{\mathrm{A}})$. In the case of nondegenerate semiconductors, furthermore, $p(T)$ is described as (16)

$$p(T) = N_{\mathrm{V}}(T) \exp\left(-\frac{\Delta E_{\mathrm{F}}(T)}{kT}\right), \qquad [8]$$

where

$$N_{\mathrm{V}}(T) = N_{\mathrm{V0}} k^{3/2} T^{3/2} \qquad [9]$$

and

$$N_{\mathrm{V0}} = 2\left(\frac{2\pi m_{\mathrm{h}}^*}{h^2}\right)^{3/2}. \qquad [10]$$

Substituting Eq. 7 for one of the two $p(T)$ in Eq. 6 and substituting Eq. 8 for the other $p(T)$ in Eq. 6 yield

$$H(T,E_{\mathrm{ref}}) = \frac{N_{\mathrm{A}}}{kT} \exp\left(-\frac{\Delta E_{\mathrm{A}} - E_{\mathrm{ref}}}{kT}\right) I(\Delta E_{\mathrm{A}}) - \frac{N_{\mathrm{D}} N_{\mathrm{V0}}}{kT} \exp\left(\frac{E_{\mathrm{ref}} - \Delta E_{\mathrm{F}}(T)}{kT}\right), \qquad [11]$$

where

$$I(\Delta E_{\mathrm{A}}) = N_{\mathrm{V0}} \exp\left(\frac{\Delta E_{\mathrm{A}} - \Delta E_{\mathrm{F}}(T)}{kT}\right) F(\Delta E_{\mathrm{A}}). \qquad [12]$$

The function

$$\frac{N_A}{kT}\exp\left(-\frac{\Delta E_A - E_{ref}}{kT}\right) \quad [13]$$

in Eq. 11 has a peak value of $N_A \exp(-1)/kT_{peak}$ at a peak temperature

$$T_{peak} = \frac{\Delta E_A - E_{ref}}{k}. \quad [14]$$

It is clear from Eq. 14 that E_{ref} can shift the peak of $H(T, E_{ref})$ within the temperature range of the measurement. Although the actual T_{peak} of $H(T, E_{ref})$ is slightly different from T_{peak} calculated by Eq. 14 due to the temperature dependence of $I(\Delta E_A)$, we can easily determine the accurate values of N_A and ΔE_A from the peak of the experimental $H(T, E_{ref})$, using a personal computer. The Windows application software for FCCS can be freely downloaded at our web site (http://www.osakac.ac.jp/labs/matsuura/).

EXPERIMENT

A 2-μm-thick Mg-doped GaN epilayer on undoped GaN buffer layer/sapphire, a 1.7-μm-thick Al-implanted 4H-SiC layer on an n-type 4H-SiC epilayer, a 400-μm-thick Al-doped 6H-SiC wafer with a resistivity of 1.4 Ωcm at room temperature, and a 4.9-μm-thick 6H-SiC epilayer on n-type 6H-SiC substrate were used. The Mg concentration (C_{Mg}) determined by secondary ion mass spectroscopy was 2×10^{19} cm^{-3}, while the Al concentration (C_{Al}) in the Al-implanted layer, which was calculated by the Monte Carlo simulation program of the stopping and range of ions in matter (21), was 1×10^{19} cm^{-3}. The value of $N_A - N_D$ in the heavily Al-doped 6H-SiC, determined by the capacitance-voltage (C-V) characteristics of the Schottky barrier junction formed using this 6H-SiC wafer, was 4.2×10^{18} cm^{-3}, and the designed Al-doping density in the lightly Al-doped 6H-SiC epilayer was 6×10^{16} cm^{-3}. They were cut into small pieces, and ohmic metal was deposited on four corner of the surface. $p(T)$ was obtained from Hall-effect measurements in van der Pauw configuration in a magnetic field of 1.4 T using a modified MMR Technologies' Hall system.

RESULTS AND DISCUSSION

Hall-Effect Measurements

Figure 1 shows $p(T)$ for Mg-doped GaN (circles), Al-implanted 4H-SiC (triangles), heavily Al-doped 6H-SiC (squares), and lightly Al-doped 6H-SiC (down triangles). Figure 2 depicts $\Delta E_F(T)$ for these samples, which are calculated by (16)

$$\Delta E_F(T) = kT \ln\left[\frac{N_V(T)}{p(T)}\right]. \qquad [15]$$

Since ΔE_A of Mg in GaN is reported to be approximately 150 meV (1) and ΔE_A of Al in 4H-SiC and 6H-SiC are approximately 180 meV (2), the values of $\Delta E_F(T)$ for the samples except the lightly Al-doped 6H-SiC are lower than these ΔE_A at all temperatures, indicating that the excited states in these samples affect $p(T)$ strongly.

FCCS Analysis

Mg-Doped GaN Epilayer. Using FCCS, the values of ΔE_A and N_A are determined from $p(T)$. Figure 3 shows $H(T, E_{ref})$ with $E_{ref} = 0.237$ eV for Mg-doped GaN. The circles represent the experimental $H(T, E_{ref})$, which is calculated by Eq. 6. Since only one peak seems to appear in this figure, this epilayer may include only one type of acceptor species. The peak temperature and value of this FCCS signal are 284.6 K and 5.5×10^{43} $cm^{-6}eV^{-2.5}$. From this peak, the values of N_A, ΔE_A and N_D are determined as 2.1×10^{20} cm^{-3}, 154 meV, and 2.2×10^{18} cm^{-3} for $f_{FD}(\Delta E_A)$, respectively. The determined value of N_A is higher by 10 than C_{Mg} of 2×10^{19} cm^{-3}, indicating that this N_A is not reliable because N_A is the concentration of Mg atoms located at the substitutional sites of Ga in GaN and C_{Mg} is the concentration of Mg atoms in this epilayer. In the case of $f(\Delta E_A)$, the values of N_A, ΔE_A and N_D are

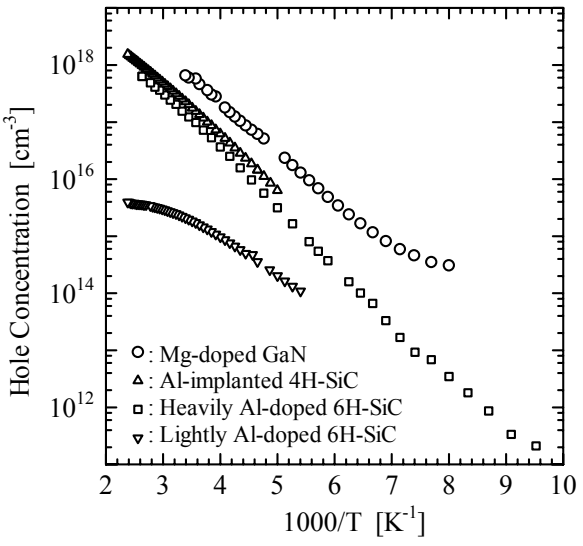

Fig. 1 Experimental $p(T)$.

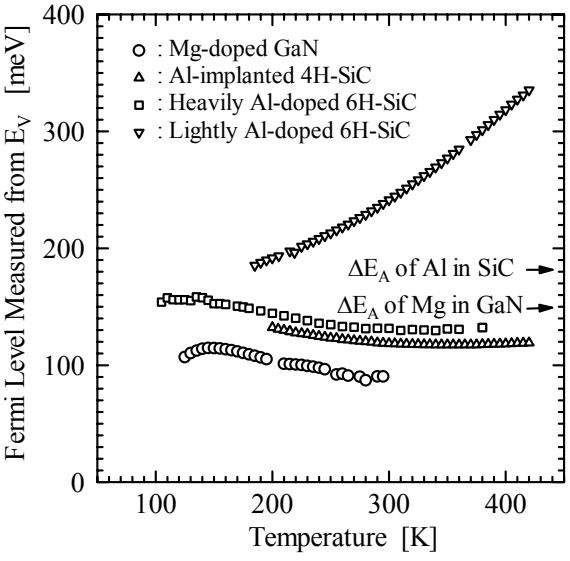

Fig. 2 Experimental $\Delta E_F(T)$.

determined as 8.9×10^{18} cm^{-3}, 149 meV, and 1.5×10^{17} cm^{-3}, respectively. Since this N_A is lower than C_{Mg}, it is found that the distribution function including the effect of the excited states of acceptors is suitable for determining N_A and ΔE_A from $p(T)$. Moreover, approximately 45 % of Mg atoms in this epilayer is found to act as an acceptor, where this epilayer was annealed at 800 °C in a N_2 atmosphere for 20 min.

The broken and solid lines in Fig. 3 represent the $H(T,E_{ref})$ simulations for $f_{FD}(\Delta E_A)$ and $f(\Delta E_A)$ using Eq. 11 with the corresponding values of N_A, ΔE_A and N_D as well as $\Delta E_F(T)$ calculated using Eq. 15 by interpolating the experimental $p(T)$ with a cubic smoothing natural spline function at intervals of 0.1 K. Since the solid line is in better agreement with the experimental $H(T,E_{ref})$ than the other, the excited states of acceptors obviously affect $p(T)$.

The circles, and broken and solid lines in Fig. 4 represent the experimental $p(T)$ and two $p(T)$ simulations using the values determined using $f_{FD}(\Delta E_A)$ and $f(\Delta E_A)$, respectively. Because the $p(T)$ simulation using $f(\Delta E_A)$ is very close to the $p(T)$ simulation using $f_{FD}(\Delta E_A)$, the solid line overlaps with the broken line. Since both the $p(T)$ simulations coincide with the experimental $p(T)$, moreover, it is difficult to determine which distribution function is suitable for determining N_A and ΔE_A from a curve fit of Eqs. 7 and 8 to $p(T)$.

Al-Implanted 4H-SiC Layer. The triangles in Fig. 5 represent the experimental $H(T,E_{ref})$ with $E_{ref}=0.231$ eV for Al-implanted 4H-SiC. Since only one peak appears in this figure, this epilayer includes only one type of acceptor species. The peak temperature and value of this FCCS signal are 381.8 K and 5.9×10^{42} cm^{-6}eV$^{-2.5}$. From this peak, N_A, ΔE_A and N_D are determined as 4.9×10^{19} cm^{-3}, 157 meV, and 2.5×10^{18} cm^{-3} for $f_{FD}(\Delta E_A)$, respectively. The determined N_A is higher by 5 than

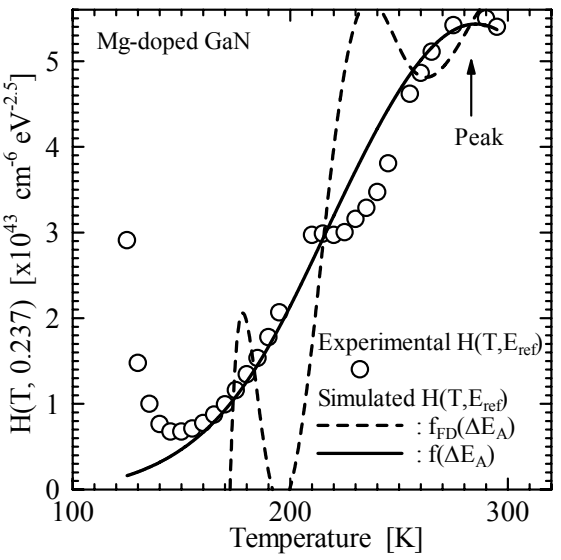

Fig. 3 FCCS signals .

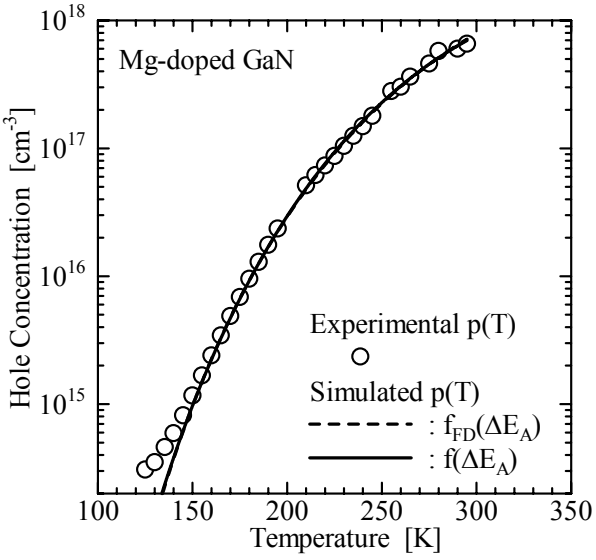

Fig. 4 $p(T)$ simulations.

C_{Al} of 1×10^{19} cm^{-3}, indicating that this N_A is not reliable because N_A is the concentration of Al atoms located at the substitutional sites of Si in SiC (22,23). In the case of $f(\Delta E_A)$, the values of N_A, ΔE_A and N_D are determined as 1.2×10^{19} cm^{-3}, 177 meV, and 2.3×10^{17} cm^{-3}, respectively. Since this N_A is nearly equal to C_{Al}, $f(\Delta E_A)$ is suitable for determining N_A and ΔE_A from $p(T)$. Moreover, it is found that almost all Al atoms in this Al-implanted layer act as an acceptor. Since this layer was Al-implanted at 1000 °C and annealed at 1575 °C in an Ar atmosphere for 1 h, the high-temperature implantation and high-temperature annealing are necessary to the activation of implanted Al atoms.

The broken and solid lines in Fig. 5 represent the $H(T,E_{ref})$ simulations for $f_{FD}(\Delta E_A)$ and $f(\Delta E_A)$ using Eq. 11 with the corresponding values of N_A, ΔE_A and N_D as well as $\Delta E_F(T)$ calculated using Eq. 15 by interpolating the experimental $p(T)$ with a cubic smoothing natural spline function at intervals of 0.1 K. Since the solid line is in better agreement with the experimental $H(T,E_{ref})$ than the other, it is proved that the excited states of acceptors affect $p(T)$.

Heavily Al-Doped 6H-SiC Wafer. The squares in Fig. 6 represent the experimental $H(T,E_{ref})$ with $E_{ref}=0.248$ eV for heavily Al-doped 6H-SiC. Since only one peak appears in this figure, this epilayer includes only one type of acceptor species. The peak temperature and value of this FCCS signal are 353.9 K and 4.1×10^{42} cm^{-6}eV$^{-2.5}$. From this peak, N_A, ΔE_A and N_D are determined as 2.5×10^{19} cm^{-3}, 180 meV, and 7.3×10^{17} cm^{-3} for $f_{FD}(\Delta E_A)$, respectively. The determined N_A-N_D is higher by 6 than N_A-N_D of 4.2×10^{18} cm^{-3} determined from the C-V characteristics of the Schottky barrier diode, indicating that this N_A is not reliable. In the case of $f(\Delta E_A)$, the values of N_A, ΔE_A and N_D are determined as

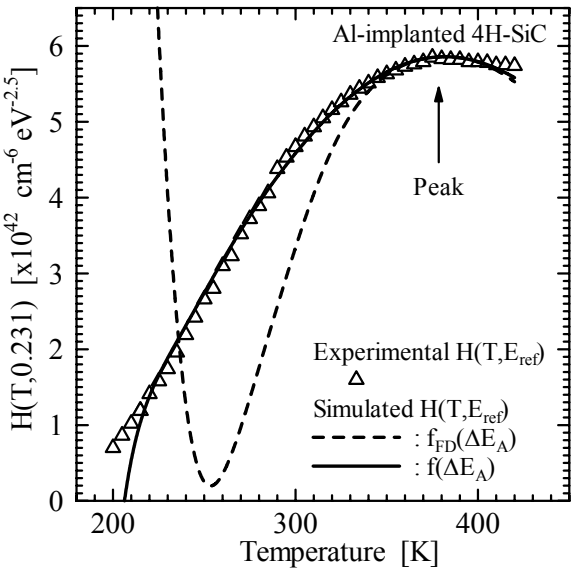

Fig. 5 FCCS signals.

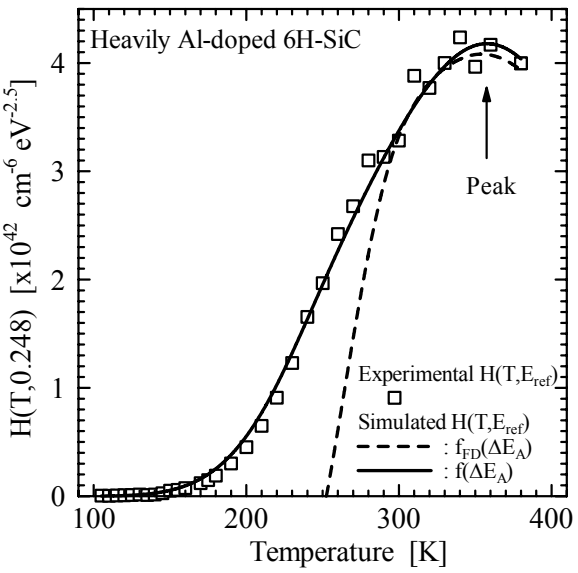

Fig. 6 FCCS signals.

3.2×10^{18} cm^{-3}, 180 meV, and 9.0×10^{16} cm^{-3}, respectively. Judging from the value determined from the C-V characteristics, this N_A is reasonable.

The broken and solid lines in Fig. 6 represent the $H(T,E_{ref})$ simulations for $f_{FD}(\Delta E_A)$ and $f(\Delta E_A)$ using Eq. 11 with the corresponding values of N_A, ΔE_A and N_D as well as $\Delta E_F(T)$ calculated using Eq. 15 by interpolating the experimental $p(T)$ with a cubic smoothing natural spline function at intervals of 0.1 K. Since the solid line is in better agreement with the experimental $H(T,E_{ref})$ than the other, it is demonstrated that the excited states of acceptors affect $p(T)$ strongly.

Lightly Al-Doped 6H-SiC Epilayer. The down triangles in Fig. 7 represent the experimental $H(T,E_{ref})$ with $E_{ref}=0$ eV for lightly Al-doped 6H-SiC. Since only one peak appears in this figure, this epilayer includes only one type of acceptor species. The peak temperature and value of this FCCS signal are 364.3 K and 6.8×10^{34} cm^{-6}eV$^{-2.5}$. From this peak, N_A, ΔE_A and N_D are determined as 4.9×10^{15} cm^{-3}, 199 meV, and 5.5×10^{14} cm^{-3} for $f_{FD}(\Delta E_A)$, respectively, and 4.1×10^{15} cm^{-3}, 212 meV, and 1.0×10^{14} cm^{-3} for $f(\Delta E_A)$, respectively. Both N_A are close to the designed Al-doping density of 6×10^{15} cm^{-3}.

The broken and solid lines in Fig. 7 represent the $H(T,E_{ref})$ simulations for $f_{FD}(\Delta E_A)$ and $f(\Delta E_A)$ using Eq. 11 with the corresponding values of N_A, ΔE_A and N_D as well as $\Delta E_F(T)$ calculated using Eq. 15 by interpolating the experimental $p(T)$ with a cubic smoothing natural spline function at intervals of 0.1 K. Both the lines are in good agreement with the experimental $H(T,E_{ref})$. Moreover, the $p(T)$ simulation using $f(\Delta E_A)$ is very close to the $p(T)$ simulation using $f_{FD}(\Delta E_A)$, and both the $p(T)$ simulations coincide with the experimental $p(T)$. These results indicate that

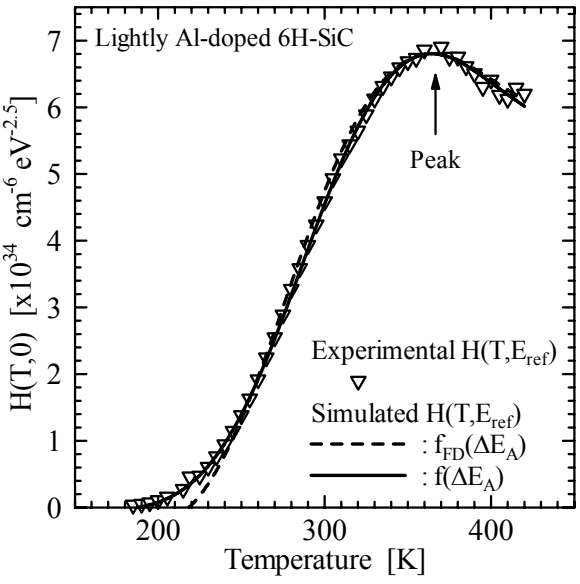

Fig. 7 FCCS signals.

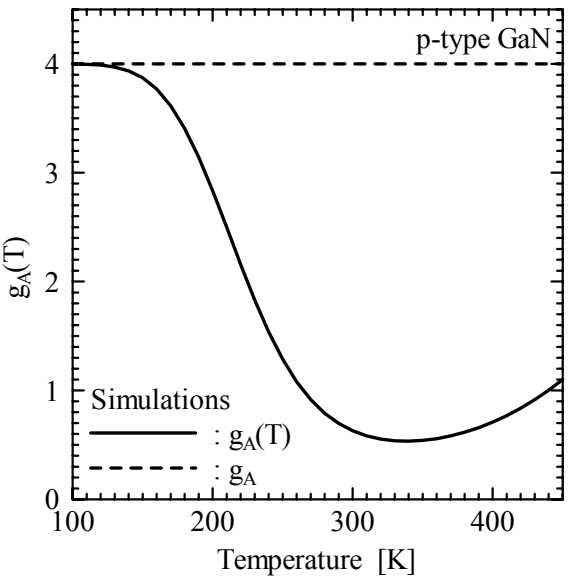

Fig. 8 $g_A(T)$ simulation.

both of $f_{FD}(\Delta E_A)$ and $f(\Delta E_A)$ can lead to reliable values for N_A and ΔE_A when $\Delta E_F(T)$ is far from E_V.

Influence of Excited States of Acceptors on Their Ionization Efficiency

Mg-Doped GaN. Figure 8 shows $g_A(T)$ in Eq. 3 for p-type GaN. It is found that $g_A(T)$ in $f(\Delta E_A)$ at >100 K is smaller than g_A of 4 in $f_{FD}(\Delta E_A)$. We investigate how this smaller $g_A(T)$ affect the ionization efficiency of acceptors.

Figure 9 depicts the temperature dependencies of the ionized acceptor densities $N_A^-(T)$ simulated with the same values of N_A, ΔE_A and N_D for $f_{FD}(\Delta E_A)$ (broken line) and $f(\Delta E_A)$ (solid line). Both the $N_A^-(T)$ are constant and equal to 1.5×10^{17} cm^{-3} at <170 K, because some of acceptors are negatively charged for the ionization of all the donors. On the other hand, $N_A^-(T)$ for $f(\Delta E_A)$ is higher than $N_A^-(T)$ for $f_{FD}(\Delta E_A)$ at >170 K, because $g_A(T)$ is lower than 4. For example, $N_A^-(T)$ for $f(\Delta E_A)$ is higher by 2 than $N_A^-(T)$ for $f_{FD}(\Delta E_A)$ at 300 K. Therefore, it is found that the excited states enhance the ionization efficiency of Mg acceptors.

Al-Doped 6H-SiC. Figure 10 shows $g_A(T)$ for p-type 6H-SiC. $g_A(T)$ in $f(\Delta E_A)$ at >140 K is smaller than g_A of 4 in $f_{FD}(\Delta E_A)$. Since $g_A(T)$ for the lightly Al-doped 6H-SiC is the same as $g_A(T)$ for the heavily Al-doped 6H-SiC, we compare $N_A^-(T)$ for the lightly Al-doped 6H-SiC with $N_A^-(T)$ for the heavily Al-doped 6H-SiC.

Figure 11 shows $N_A^-(T)$ simulated with the same values of N_A, ΔE_A and N_D for $f_{FD}(\Delta E_A)$ (broken line) and $f(\Delta E_A)$ (solid line) for the heavily Al-doped sample. Figure 12 depicts $N_A^-(T)$ simulated with the same values of N_A, ΔE_A and N_D for $f_{FD}(\Delta E_A)$ (broken line) and $f(\Delta E_A)$ (solid line) for the lightly Al-doped sample.

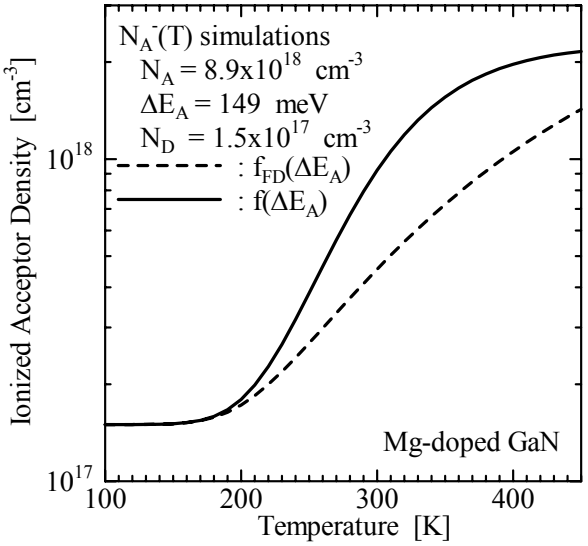

Fig. 9. Ionized acceptor density.

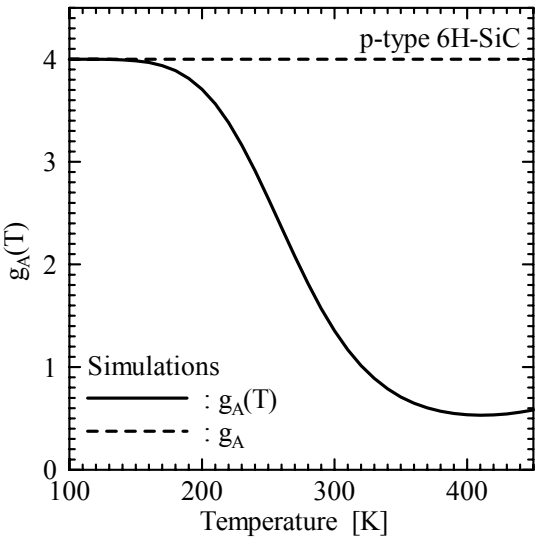

Fig. 10 $g_A(T)$ simulation.

$N_A^-(T)$ for $f(\Delta E_A)$ is close to $N_A^-(T)$ for $f_{FD}(\Delta E_A)$ in the lightly doped sample, while $N_A^-(T)$ for $f(\Delta E_A)$ is higher than $N_A^-(T)$ for $f_{FD}(\Delta E_A)$ in the heavily doped sample. As a consequence, the excited states undoubtedly enhance the ionization efficiency of acceptors when $\Delta E_F(T)$ is located between E_V and ΔE_A. This is because a lot of holes exist at the excited states in the heavily doped case.

CONCLUSIONS

We investigated a distribution function suitable for deep acceptors in p-type wide bandgap semiconductors. In order to determine N_A and ΔE_A from $p(T)$ for the heavily doped samples, the distribution function including the influence of the excited states of acceptors was found to be necessary. In other words, it was proved that the excited states of deep acceptors affected $p(T)$. Moreover, the excited states obviously enhanced the ionization efficiency of deep acceptors in heavily doped p-type wide bandgap semiconductors.

ACKNOWLEDGMENTS

The author would like to thank Prof. T. Suzuki of Nippon Institute of Technology for the GaN sample preparation, and Dr. H. Sugiyama of the Mitsubishi Electric Corp. for the Al-implanted 4H-SiC sample preparation. This work was partially supported by the Academic Frontier Promotion Projects of the Ministry of Education, Culture, Sports, Science and Technology, and it was also partially supported by the R&D Association of Future Electron Devices (FED) and the New Energy and Industrial Technology

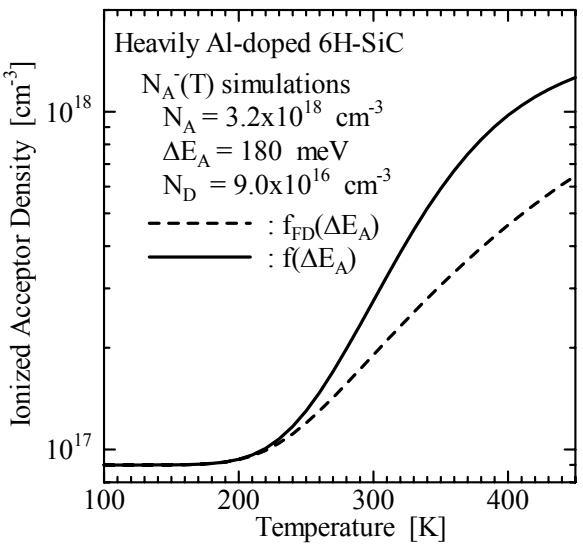

Fig. 11 Ionized acceptor density.

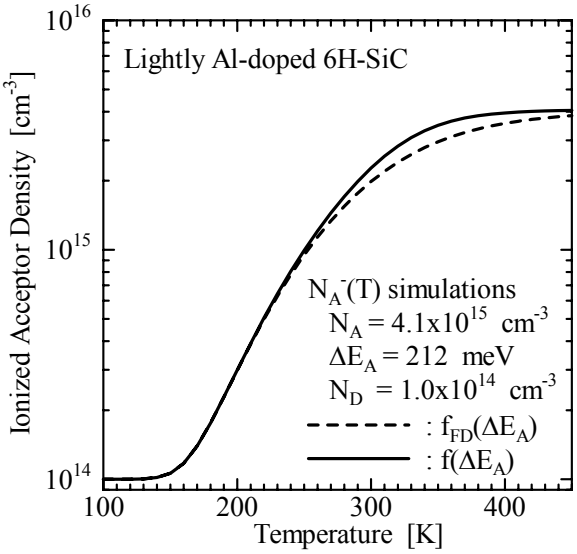

Fig. 12 Ionized acceptor density.

Development Organization (NEDO).

REFERENCES

1. H. Morkoc, *Nitride Semiconductors and Devices*, chap. 7, Springer, Berlin (1999).
2. M. Ikeda, H. Matsunami, and T. Tanaka, *Phys. Rev.,* **B22**, 2842 (1980).
3. Y. P. Yu and M. Cardona, *Fundamentals of Semiconductors: Physics and Materials Properties*, 2nd ed., chap. 4, Springer, Berlin (1999).
4. H. Matsuura, *New J. Phys.*, **4**, 12.1 (2002) [http://www.hjp.org/].
5. H. Matsuura, D. Katsuya, T. Ishida, S. Kagamihara, K. Aso, H. Iwata, T. Aki, S-W. Kim, T. Shibata, and T. Suzuki, *Phys. Status Solidi*, **C0**, 2214 (2003).
6. H. Matsuura, K. Sugiyama, K. Nishikawa, T. Nagata, and N. Fukunaga, *J. Appl. Phys.*, **94**, 2234 (2003).
7. H. Matsuura, *J. Appl. Phys.*, **95**, 4213 (2004).
8. H. Matsuura, K. Aso, S. Kagamihara, H. Iwata, and T. Ishida, *Appl. Phys. Lett.*, **83**, 4981 (2003).
9. H. Matsuura and K. Sonoi, *Jpn. J. App. Phys.*, **35**, L555 (1996).
10. H. Matsuura, *Jpn. J. Appl. Phys.*, **36**, 3541 (1997).
11. H. Matsuura, Y. Uchida, T. Hisamatsu, and S. Matsuda, *Jpn. J. Appl. Phys.*, **37**, 6034 (1998).
12. H. Matsuura, T. Kimoto, and H. Matsunami, *Jpn. J. Appl. Phys.*, **38**, 4013 (1999).
13. H. Matsuura, Y. Uchida, N. Nagai, T. Hisamatsu, T. Aburaya, and S. Matsuda, *Appl. Phys. Lett.*, **76**, 2092 (2000).
14. H. Matsuura, Y. Masuda, Y. Chen, and S. Nishino, *Jpn. J Appl. Phys.*, **39**, 5069 (2000).
15. H. Matsuura, K. Morita, K. Nishikawa, T. Mizukoshi, M. Segawa, and W. Susaki, *Jpn. J. Appl. Phys.*, **41**, 496 (2002).
16. S. M. Sze, *Physics of Semiconductor Devices*, 2nd ed. chap. 1, Wiley, New York (1981).
17. D. V. Lang, *J. Appl. Phys.*, **45**, 3023 (1974).
18. H. Okushi, *Philos. Mag.*, **B52**, 33 (1985).
19. H. Matsuura, *J. Appl. Phys.*, **64**, 1964 (1988).
20. H. Matsuura, T. Hase, Y. Sekimoto, M. Uchida, and M. Simizu, *J. Appl. Phys.*, **91**, 2085 (2002).
21. J. P. Biersack and L. Haggmark, *Nucl. Instrum. Methods*, **174**, 257 (1980).
22. S. G. Weber, *Phys. Status Solidi*, **A162**, 95 (1997).
23. T. Troffer, M. Schadt, T. Frank, H. Ito, G. Pensl, J. Heindl, H. P. Strunk, and M. Maier, *Phys. Status Solidi*, **A162**, 162 (1997).